



**HAL**  
open science

## Short-term to decadal-scale onshore bar migration and shoreline changes in the vicinity of a megatidal ebb delta

Nicolas Robin, F. Levoy, O. Monfort, Edward J. Anthony

### ► To cite this version:

Nicolas Robin, F. Levoy, O. Monfort, Edward J. Anthony. Short-term to decadal-scale onshore bar migration and shoreline changes in the vicinity of a megatidal ebb delta. *Journal of Geophysical Research: Earth Surface*, 2009, 114 (F4), pp.f04024. 10.1029/2008JF001207 . hal-00489405

**HAL Id: hal-00489405**

**<https://hal.science/hal-00489405>**

Submitted on 22 Jun 2021

**HAL** is a multi-disciplinary open access archive for the deposit and dissemination of scientific research documents, whether they are published or not. The documents may come from teaching and research institutions in France or abroad, or from public or private research centers.

L'archive ouverte pluridisciplinaire **HAL**, est destinée au dépôt et à la diffusion de documents scientifiques de niveau recherche, publiés ou non, émanant des établissements d'enseignement et de recherche français ou étrangers, des laboratoires publics ou privés.

Copyright

## Short-term to decadal-scale onshore bar migration and shoreline changes in the vicinity of a megatidal ebb delta

Nicolas Robin,<sup>1</sup> Franck Levoy,<sup>1</sup> Olivier Monfort,<sup>1</sup> and Edward Anthony<sup>2</sup>

Received 24 November 2008; revised 10 June 2009; accepted 14 September 2009; published 17 December 2009.

[1] Swash bar development has been well documented from coasts with low to moderate tidal ranges, while studies of the effects of these forms on the morphology and dynamics of the adjacent shore in large tide range environments are rare. The analysis of sequential vertical aerial photographs was combined with field work in order to highlight the effects of swash bar development on the adjacent shoreline in the vicinity of a megatidal inlet (mean spring tidal range of 11 m). Swash bars are observed to form on the ebb tidal delta and to migrate landward before welding onto the coast. A close relationship was noticed between the position of the swash bar and shoreline dynamics. The bar protects the shore against wave attack in a sedimentary system controlled by longshore transport. This protective role is, however, modulated by the large tidal range. As the bar migrates upward toward the high-tide level and the subaerial beach, it develops morphologically into a transverse form that acts as a cross-shore obstacle to longshore sediment transport, thus resulting in shoreline accretion updrift and in strong erosion downdrift. This disturbance may persist for years because of the relatively slow speed of movement of the bar at this stage, an aspect characteristic of large tide range environments. This pattern of behavior differs fundamentally from that documented in the literature where the perturbation of the longshore sediment transport occurs over shorter periods. An original conceptual model of swash bar morphodynamics and repercussions on the adjacent shoreline for this megatidal environment is proposed.

**Citation:** Robin, N., F. Levoy, O. Monfort, and E. Anthony (2009), Short-term to decadal-scale onshore bar migration and shoreline changes in the vicinity of a megatidal ebb delta, *J. Geophys. Res.*, 114, F04024, doi:10.1029/2008JF001207.

### 1. Introduction

[2] Ebb tidal deltas in micromesotidal settings commonly exhibit swash bars ranging in length from 300 m to several km [Oertel, 1972; Hayes, 1975] that are built by wave-induced accumulation of sand [Hine, 1975]. Although ebb delta bars are a major component of the morphology of tidal inlets and of the shoreline sediment budget [Oertel, 1977], albeit with patterns of development that vary considerably along wave and tide range gradients [Davis, 2004], the relationships between shoreline morphological evolution and landward swash bar migration are not well established. Swash bars tend to migrate landward under surf bores and swash processes at rates that can be quite high, but extremely variable, ranging from 64 to 86 m yr<sup>-1</sup> [Smith and FitzGerald, 1994] to 133–327 m yr<sup>-1</sup> [FitzGerald, 1984; Gaudio and Kana, 2001], but an exceptional rate of 46 m month<sup>-1</sup> has also been reported [Balouin et al., 2001, 2004]. Their migration and welding onto the adjacent beaches generally result in rapid, localized shoreline

progradation, with reported values of 10 to over 400 m on both sides of inlets [Hine, 1979; FitzGerald, 1982, 1984, 1988; FitzGerald et al., 1984; Fenster and Dolan, 1996; Kana et al., 1999; Gaudio and Kana, 2001; Borrelli and Wells, 2003; Kana and McKee, 2003]. The shoreward migration process in such wave-dominated to mixed energy (wave tidal) settings may involve coalescence of individual bars to form large complex bars (300 m to several km long) just before welding onto the shoreline [Hine, 1975; Aubrey and Speer, 1984; FitzGerald, 1984, 1988; FitzGerald et al., 1984, 2000; Kana et al., 1999; Borrelli and Wells, 2003]. Such welding sometimes results in the formation of large hook spits [FitzGerald, 1984; Gaudio and Kana, 2001]. The bar welding mechanism can, thus, be an extremely important form of natural beach nourishment, attaining, in some cases, several millions of m<sup>3</sup> in the course of a single welding event [Kana et al., 1999]. Where the ebb delta is devoid of swash bars, shoreline erosion can be observed on the downdrift side of the inlet [FitzGerald, 1984]. The pattern of shoreline erosion and deposition in the vicinity of such inlets is controlled by cycles of ebb tidal delta growth (swash bar formation) and decay (bar welding) that last from 4 to 8 years on the east coast of the United States [Gaudio and Kana, 2001].

[3] The dynamics of swash bar impingement on the shore involve morphodynamic feedbacks among waves, long-

<sup>1</sup>Laboratoire Morphodynamique Continentale et Côtière, UMR 6143, Université de Caen, CNRS, Caen, France.

<sup>2</sup>Laboratoire d'Océanologie et de Géosciences, UMR 8187, Université du Littoral Côte d'Opale, CNRS, Wimereux, France.

shore sediment transport, bar morphology, morphological relaxation, and inlet processes, and have formed the basis for morphosedimentary models depicting the final stages of swash bar attachment to the beach [e.g., *Hine*, 1979; *Kana et al.*, 1999]. The conceptual model proposed by *Kana et al.* [1999] comprises three stages. Stage one depicts an offshore bar isolated from the rest of the swash platform near the downdrift limits of the ebb-tidal delta. In stage two, the bar migrates landward and starts getting attached to the beach face. Beach erosion typically occurs adjacent to both sides of the bar, and accretion continues directly in its lee. The third and final stage involves alongshore spreading of the bar in either direction from the point of attachment. Typically, a bulge in the shoreline persists where the bar attaches. In the *Kana et al.* [1999] model, bar attachment introduces a new sediment supply source to the beach littoral drift system [see also *Kana et al.*, 1985]. This phase can be rapid, not exceeding, for instance, 2 years at Dewees Inlet, South Carolina [*Gaudio and Kana*, 2001]. Although not specifically addressing swash bar dynamics in relation to inlets, the berm development and ensuing beach accretion model of *Hine* [1979] is also hinged on the welding of a swash bar along the initial curvature zone of a spit, thus creating a wide, flat intertidal surface. High-tide swash processes cannot prevail over this broad intertidal feature, thus resulting in the formation of a large berm ridge or hook spit. The large intervening trough or runnel becomes inactive and slowly infills through the addition of wind-transported sand. This model is confirmed by observations reported from many other inlets [*Nummedal and Penland*, 1981; *FitzGerald*, 1982, 1984]. As *Hicks et al.* [1999] have noted, much of the work carried out thus far has focused on descriptions and conceptual models. Knowledge on the magnitude of swash bar-induced beach change and on how such change varies alongshore away from the inlet is extremely sparse. Furthermore, aspects relating to the morphology and dynamics of these bars, and to the impact of these features on the coastline in very large tide range settings (spring tidal ranges > 8 m) are unknown.

[4] The purpose of this paper is to describe the short- to long-term (order of months to > 10 years) erosional-depositional trends that occur along the shoreline adjacent to a megatidal ebb tidal delta, and to demonstrate their links with swash bar position and morphodynamics. The essentially mesoscale to macroscale approach adopted here reposes on the use of vertical aerial photographs, but is supported by short- to medium-term monitoring of beach and bar topography and bar-shoreline morphodynamics. The paper complements recent work on the surf and swash processes involved in megatidal bar mobility [*Robin et al.*, 2009]. The discussion of the results is followed by the proposal of a conceptual model of swash bar development and interactivity with the shoreline for a megatidal environment. The term megatidal has been proposed to cover environments with spring tidal ranges exceeding 8 m [*Levoy et al.*, 2000].

## 2. Study Area

[5] The west Cotentin coast in the central English Channel is a low-lying linear sandy coast comprising eight small tidal inlets (Figure 1). This coast is a fine example of a

megatidal environment [*Levoy et al.*, 2000], where the maximum spring tidal range reaches 15 m, among the highest in the world. The offshore area is characterized by very complex hydrodynamic conditions. Mean currents, measured at Les Nattes (Figure 1), are parallel to the coast during most of the tidal cycle, flow northward at high tide and southward at low tide, and can reach  $1 \text{ m}\cdot\text{s}^{-1}$  near high and low water [*Levoy et al.*, 2001]. Recorded wave heights at Les Nattes are less than 0.5 m 65% of the time. Wave heights larger than 1.5 m are observed only 2% of the time. The peak period is in the 5–9 s range, and reflects a mix of distant swell from the north Atlantic and locally generated wind waves. Wave propagation is complicated by the shore face bathymetry, by the Channel Islands, and by the numerous shoals, islets, rock platforms and ebb deltas, which result in considerable attenuation of wave heights [*Levoy et al.*, 2001]. Waves come mainly from a west window (waves with southwesterly to northwesterly directions represent more than 90% of the observations). The Channel Islands embayment may be viewed as a very large dissipative zone with decreasing wave heights from north to south and from west to east.

[6] The study site concerns the largest of the tidal inlets, Regnéville inlet (Figure 1), diverted by Agon Spit, a complex body that migrates to the southeast and the distal end of which exhibits several recurves (Figure 2a). The north-south littoral drift along the spit is estimated at about  $40,000 \text{ m}^3 \text{ yr}^{-1}$ , but there is evidence for counterdrift along the coast immediately downdrift of the diverted inlet, and, therefore, sediment convergence at the ebb delta platform, due to refraction [*Levoy*, 1994]. The ebb delta is a large subtidal to intertidal feature extending more than 4 km offshore. It exhibits few, relatively stable bars that are commonly linear, and of low elevation (<0.5 m high). Two to three bars of larger elevation (up to 2 m high) can be identified at any one time, on the northern part of the ebb delta. These higher bars migrate shoreward and have a highly asymmetrical transverse profile that shows alongshore uniformity. The bars exhibit three distinct morphological sections: a seaward slope, a slip face and a trough (Figures 2b and 2c). The seaward slope generally has a gentle gradient ( $\tan\beta \approx 0.02$ ) and is characterized by sand with a mean  $D_{50}$  value of 0.5 mm and by numerous shells and gravel clasts. The bars are generally shorter than those in other tidal environments, but have nearly identical cross-shore morphometric parameters [*Robin et al.*, 2007a, 2007b]. The trough is generally flat and characterized by finer sediment than the seaward slope. The  $D_{50}$  value is about 0.2 mm and the sediment is devoid of shells. *Robin and Levoy* [2005] collated data on bar volumes relative to tidal prism and showed that the mean bar volume ( $29,000 \text{ m}^3$ ) in Regnéville inlet is at least seven times smaller than that of bars in microtidal settings with inlets of comparable tidal prisms. The adjoining beaches along the west Cotentin coast can be up to 1 km wide at low tide and exhibit a typical megatidal zonation (Figure 2d) involving a high-tide beach between mean high water springs and mean high water neaps, a midtidal zone between mean high water neaps and mean low water neaps, and a low-tidal zone below mean low water neaps [*Levoy et al.*, 2000; *Robin*, 2007].

[7] The tidal range in Regnéville inlet attains 11 m at mean spring tides and 14 m during exceptional spring tides. These conditions produce a mean tidal prism of  $15.10^6 \text{ m}^3$  per tidal cycle, and a mean spring tidal prism of  $46.10^6 \text{ m}^3$

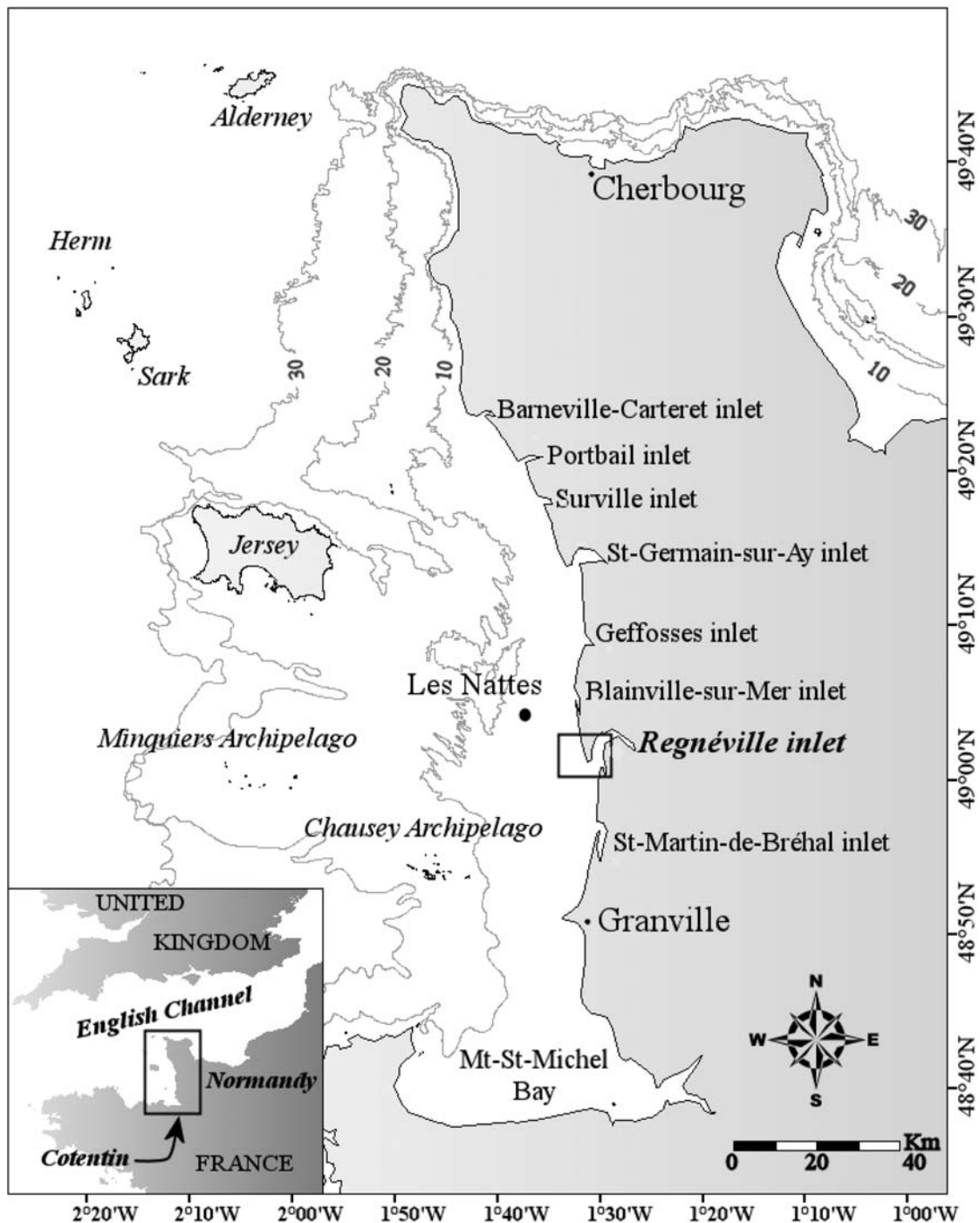


**Figure 1.** The megatidal inlets of the west Cotentin coast, in Normandy, France, and location of Regnéville inlet.

per tidal cycle. The average freshwater discharge represents only 0.6% of the mean spring tidal prism ( $10^5 \text{ m}^3$ ). The hydrodynamic conditions prevailing over one of the currently active swash bars (identified as bar 2 in text) have been described by Robin [2007] and Robin *et al.* [2007b, 2009]. High-tide water depths over the top of the bar vary significantly in the course of the fortnightly tidal cycle, ranging from 0.8 m at neaps to up to 4.5 m at springs. Significant wave heights vary markedly as waves cross the bar and as a function of the tide-influenced water depths. Wave

heights over the bar are at a maximum at high tide and decrease with the water level, in agreement with other studies on macrotidal beaches [Russell *et al.*, 1991; Voulgaris *et al.*, 1996; Levoy *et al.*, 2001; Anthony *et al.*, 2004, 2005; Reichmüth and Anthony, 2007; Sedrati and Anthony, 2007]. Wave attenuation increases as depths decrease until emersion of the crest of the bar. This wave height attenuation is less marked during spring tides than during neap tides (Figure 3). During neap tides, the crest of the bar is submerged only about 2 h. The ensuing wave attenuation is always greater

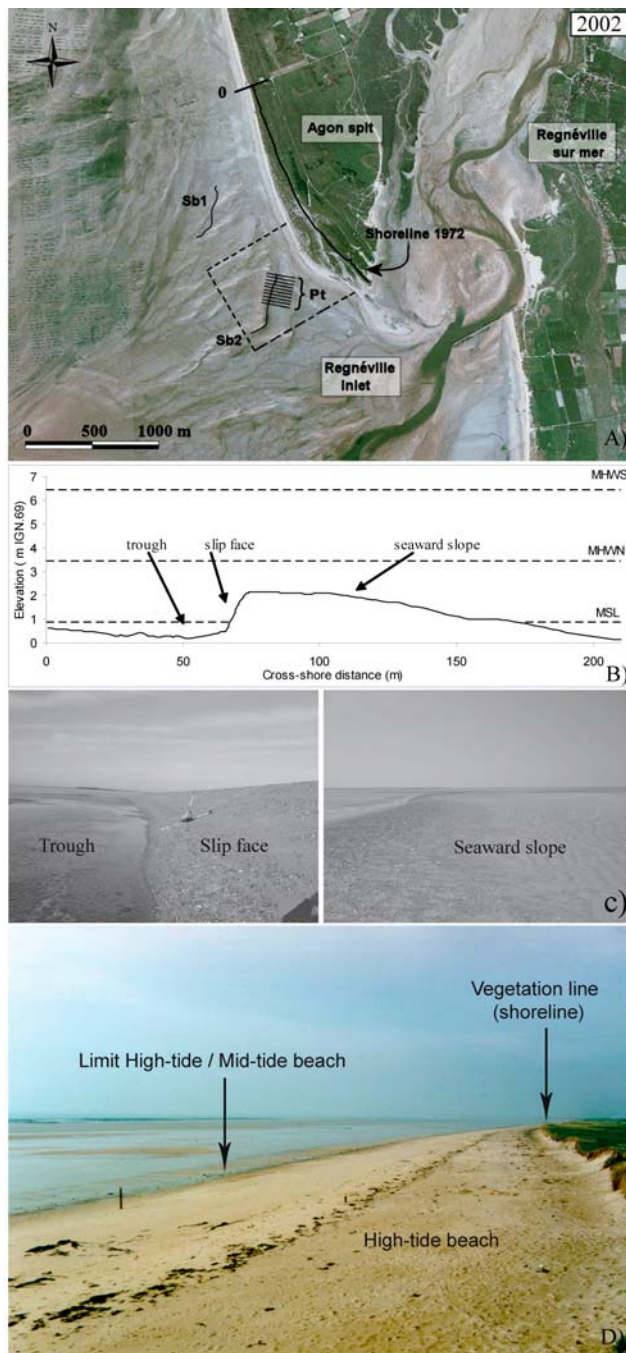


**Figure 2.** (a) A 2002 aerial photograph of Regnéville Inlet, showing locations of profile transects transverse to the currently active bar (bar 2), a  $700 \times 700$  m zone (delimited by broken lines) topographically monitored using kinematic DGPS mounted on a quad, the position of bar 1 (Sb 1) identified from a 1972 photograph, bar 2 (Sb 2), and the segment of spit shoreline (origin at 0) analyzed from the aerial photographs. (b) A typical profile of the swash bar (bar 2): MHWs, mean high water springs; MHWn, mean high water neaps; MSL, mean sea level. (c) Ground photographs of (left) swash bar 2 showing the bar slip face and (right) the top of the seaward slope. The height of the slip face is  $\sim 2$  m. (d) Ground photograph of typical megatidal beach on the west coast.

than 42%. During spring tides, the submersion time is about twice longer and attenuation of the significant wave height from 15% to about 40%.

### 3. Methods

#### 3.1. Analysis of Bar and Shoreline Variations

[8] The present study is based on the analysis, using ArcView geographic information system, of thirteen vertical aerial photographs taken by the French National Geographic Institute (IGN) from 1972 to 2002 at low tide and at scales ranging from 1/20000 to 1/30000. The photographs were digitized at a high scan resolution of 800 dpi in order to obtain images with a maximum pixel size of 2 m. Raster data were georeferenced to the orthophotograph<sup>®</sup> “Littoral 2000” (pixel size of 0.5 m) using the module Georeference<sup>®</sup> V2.2a. Once the calibration points were set, a transformation model computed the resulting mean quadratic error between the real X, Y coordinates of a point and the coordinates calculated by georeferencing. This error was always less than 2 m for the images treated, an acceptable error given the spatial scale of the study, and one that does not require overall orthorectification of the image.

[9] The crests of bars on the ebb delta, the shoreline, and the limit between the high-tide beach face and the rest of the intertidal beach were digitized on all vertical aerial photographs. Identification of bar crests was carried out from color contrasts following application of image processing tools to the photographs. Following *Moore et al.* [2003], the midpoint between the visible image-enhanced landward and seaward edge of a bar was used as a proxy for the bar crest. To analyze shoreline variability and trends, a functional definition of the shoreline is required. *Parker* [2003] has underlined the fact that the choice of the indicator is dependent on the morphological and physical characteristics of the field site, as well as on the timescale considered for the study. An ideal shoreline position indicator should be easily identified in the field and on aerial photography. Various features (biological, anthropogenic, and morphological) on the beach and backshore have been used as reference lines, including the vegetation line, bunkers, the bluff top, fore-dune foot, the beach crest, or the water line [*Boak and Turner, 2005*]. Identifying the shoreline in macromegatidal settings is complicated by the large variations in intertidal exposure of the beach and by the observation of large fluctuations in accretion of the high-tide beach [*Robin, 2007*]. This pattern of accretion is driven by storm-driven onshore migration of nearshore bars, including tidal sand ridges, and has been described from other beaches in the eastern English Channel [*Anthony et al., 2007; Aubry et al., 2009*]. To identify patterns of shoreline change due to onshore bar migration in such settings therefore also requires that fluctuations of the width of the high-tide beach are taken into account. Two indicators have, therefore, been retained here. The vegetation line has been chosen as an indicator of the shoreline. The field site of Regnéville inlet is protected from human pressures and has the advantage of having dense and easily recognizable vegetation on aerial photographs. On the west Cotentin coast, the limit between the high-tide beach and the rest of the intertidal zone corresponds to a well-defined break of slope separating a steep, dry reflective sandy high-tide beach face, sometimes

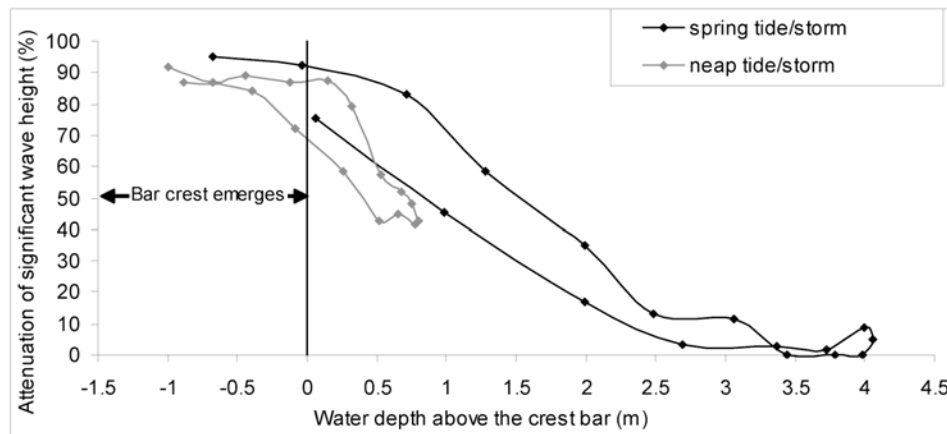


**Figure 3.** Attenuation of the significant wave heights between the seaward slope of bar 2 and the trough in the course of experiments conducted during storm conditions (neap tide, 29–30 January 2004 and spring tide, 22–23 March 2004).

comprising gravel clasts, from featureless, permanently wet, low-gradient dissipative midtide and low-tide zones (Figure 2d) [Levoy *et al.*, 2000]. This well-defined line of change was used as an indicator of the seaward limit of the high-tide beach and was carefully extracted from the aerial photographs using color contrast-enhancing tools. Once all the shorelines and limits of the high-tide beach were obtained, the next step consisted of extracting their variations over time. This was carried out using a code developed at the University of Caen [Robin, 2007; Robin and Levoy, 2007]. To this end, 120 working profiles spaced at 20 m intervals were constructed orthogonal to the oldest line. Finally, the coordinates of the shoreline position corresponding to each profile were determined from the intersection of each profile with the shoreline. By repeating this procedure for every survey, a database composed of shoreline distances from fixed points (corresponding to the working profiles) was obtained. Long-term (decadal and more) shoreline positions were measured to within a total error of  $\pm 10$  m. This range reflects errors due to inherent inaccuracies of the base map, photograph referencing and measurement errors and is similar to that reported in the literature [Crowell *et al.*, 1991; Fisher and Overton, 1994; Moore, 2000, Moore *et al.*, 2003]. This error is calculated from identified points from the orthophotograph “Littoral 2000” and from georeferenced field control points.

### 3.2. Analysis of Field Topographic Data

[10] Field monitoring of bar topography was carried out every month from November 2003 to February 2008 using kinematic Differential GPS (DGPS). The survey accuracy ( $\pm 2.5$  cm) was evaluated using control benchmarks on the beach referenced to the French Geodesic Service (IGN 69). Ten 250 m long profile transects spaced 25 m apart, transverse to the bar, were surveyed at low tide (Figure 2a). The cross-shore spacing between the measured points was less than 1 m and special attention was paid to the bar slip face. Monitoring of the beach and swash bar topography over a 700 m  $\times$  700 m zone (Figure 2a) was carried out every month between November 2003 and May 2005, then once every six months between May 2005 and February 2008, using the

same instrument mounted on a customized unit and towed by a quad vehicle, with a survey accuracy estimated at  $\pm 2.5$  cm. The topographic data sets generated by these surveys enable a good appraisal of the 3-D morphological evolution of the beach and welded bar, with an accuracy estimated at  $\pm 5$  cm. Digital elevation models were computed from the data using the Kriging interpolation method, which generates elevations on a regular grid from a weighted linear combination of values measured for neighboring points. The vegetation line was also surveyed twice a year between February 2004 and February 2008, as a complement to identification of this line on vertical aerial photographs.

## 4. Results

### 4.1. Long-Term (Greater Than Decadal-Scale) Evolution

[11] The phases of the decadal-scale pattern of swash bar-shoreline evolution in Régneville inlet are synthesized in Figure 4 from a representative selection of aerial photographs. In July 1972, a 600 m long swash bar that did not exist in an earlier, 1969, photograph appeared 400 m from the shoreline, oriented  $40^\circ$  relative to the shoreline axis. The aerial photographs between 1972 and 1977 depict a landward migration of this bar, together with almost generalized seaward advance of the limit of the high-tide beach and of the dune vegetation line representing the shoreline. Over the same period, the distal extremity of Agon spit retreated 100 m and the high-tide beach narrowed by 80 m. The landward migration of the bar culminated in the emplacement of a transverse bar morphology linked to the intertidal beach in 1977 (Figure 4b). Between 1977 and 1979, the high-tide beach updrift of the bar widened by 18 m, while the downdrift side narrowed by 15 m. Between 1979 and 1984, the bar progressively welded onto the high-tide beach. Shoreline advance was observed on the updrift side of the bar, while the downdrift side underwent a significant retreat of 75 m in 5 years. The shoreline orientation at the updrift side of the bar remained unchanged (SE), but shifted to south-southeast at the end of the spit. A hook spit formed between 1979 and 1984 in line with this new orientation (Figure 4d).

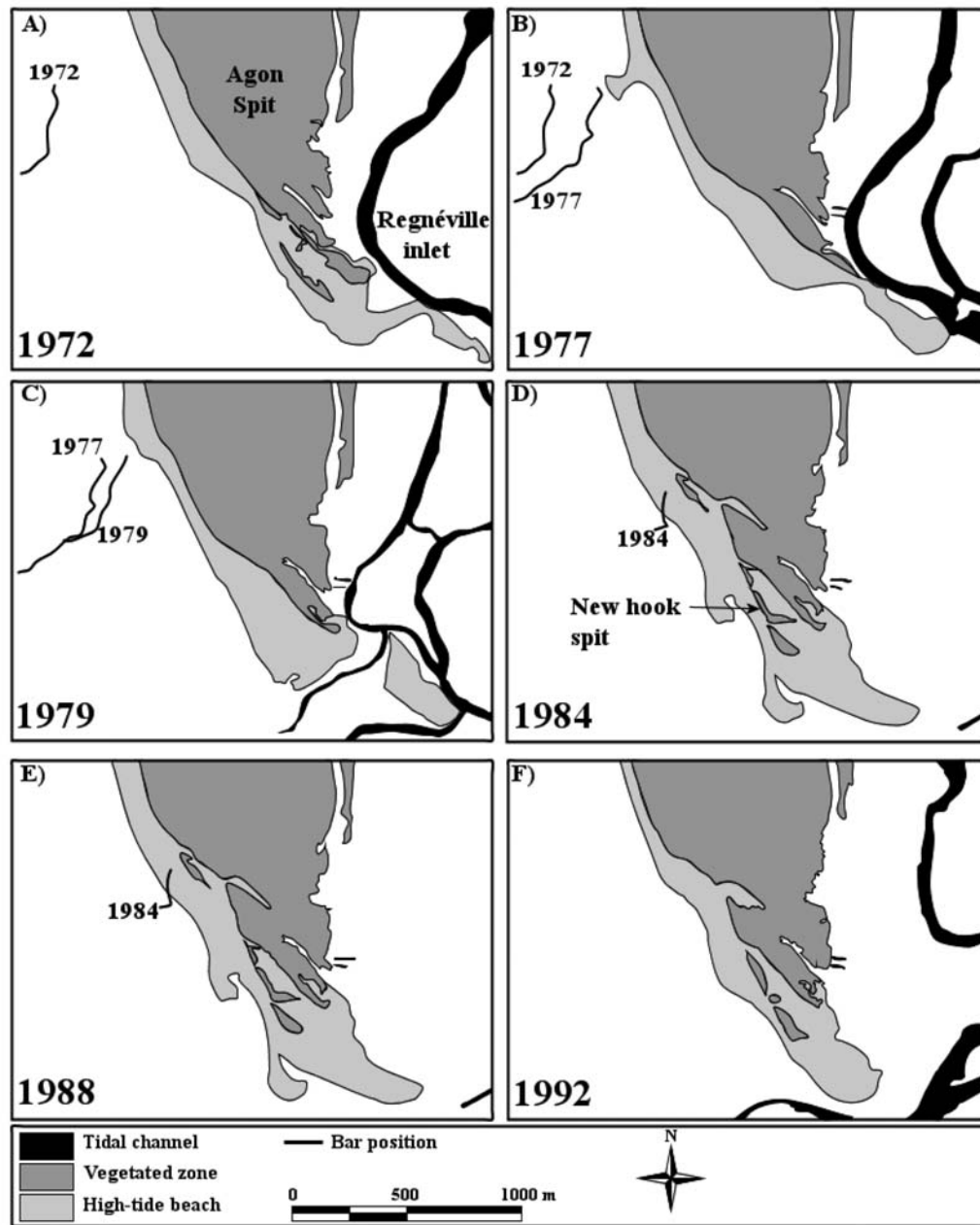


**Figure 4.** The evolution of Agon spit and successive locations of swash bar 1 between 1972 and 1992.

Until 1983, the bar moved only landward in the east-southeast direction at a constant rate of  $35.8 \text{ m yr}^{-1}$ . This migration within the intertidal zone was accompanied by a reduction in bar length from 600 m in 1972 to 183 m in 1983 when the bar welded onto the high-tide beach. The migration rate increased sharply between 1983 and 1984 to attain 118 m, this significant increase occurring just before complete welding of the bar onto the high-tide beach. An oblique aerial photograph of the field site in March 1986 shows the formation of a lateral hook along the spit (Figure 5), a feature indicative of active longshore transport in the high-tide zone toward the extremity of the spit. This hook is a product of the welding of the swash bar onto the high-tide beach. It also shows that the longshore sediment transport is not modified by the presence of the

bar in the upper part of the ebb delta. The bar welding resulted in a 100 m advance of the high-tide beach and in the isolation of a trough at the back of the lateral hook. The accretion in this zone thus succeeded an important phase of erosion of the beach observed over the 1979–1984 period prior to the initial phase of swash bar welding (Figure 5). The lateral hook moved toward the southeast and welded onto the terminal spit hook in 1990, thus resulting in regularization of the shoreline orientation (Figure 4f).

#### 4.2. Mesoscale (Order of Years) Morphological Change

[12] Aerial photographs dating back to August 1998 highlight another migrating swash bar (bar 2) (Figure 6). By June 2005, the bar had migrated to 360 m from the high-

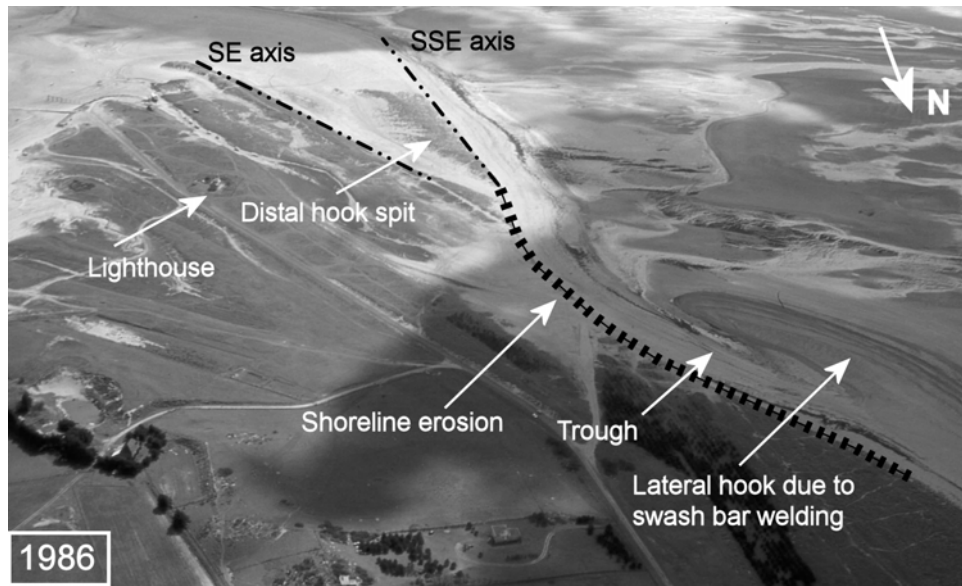


**Figure 5.** Swash bar (bar 2) and shoreline morphological features along Agon spit in March 1986. Note the welding of the swash bar along a zone of former erosion, widening of the high-tide beach, and growth of the lateral hook to the southeast, resulting in the isolation of a trough.

tide beach. It attained the midtide zone in February 2008, to assume an orientation transverse to the shore, with an angle of 40° approximately 600 m south of the 1972 position of bar 1. Bar 2 had a constant length of about 400 m between

1998 and 2002, the length decreasing thereafter. The evolution toward a transverse morphology at about the same distance to the shore as bar 1 highlights a possibly common morphodynamic pattern. The earliest field topographic

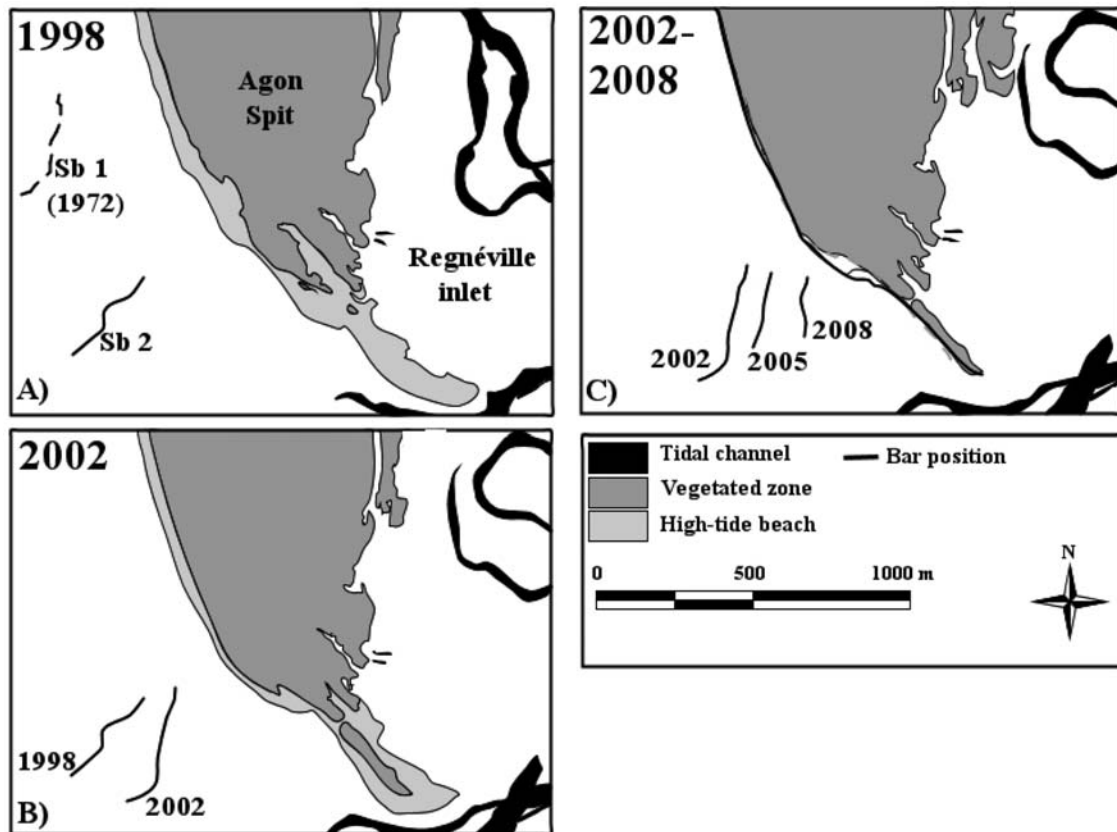


**Figure 6.** The evolution of Agon spit and successive locations of swash bar 2 between 1998 and 2008. Note the 1972 location of swash bar 1 for comparison.



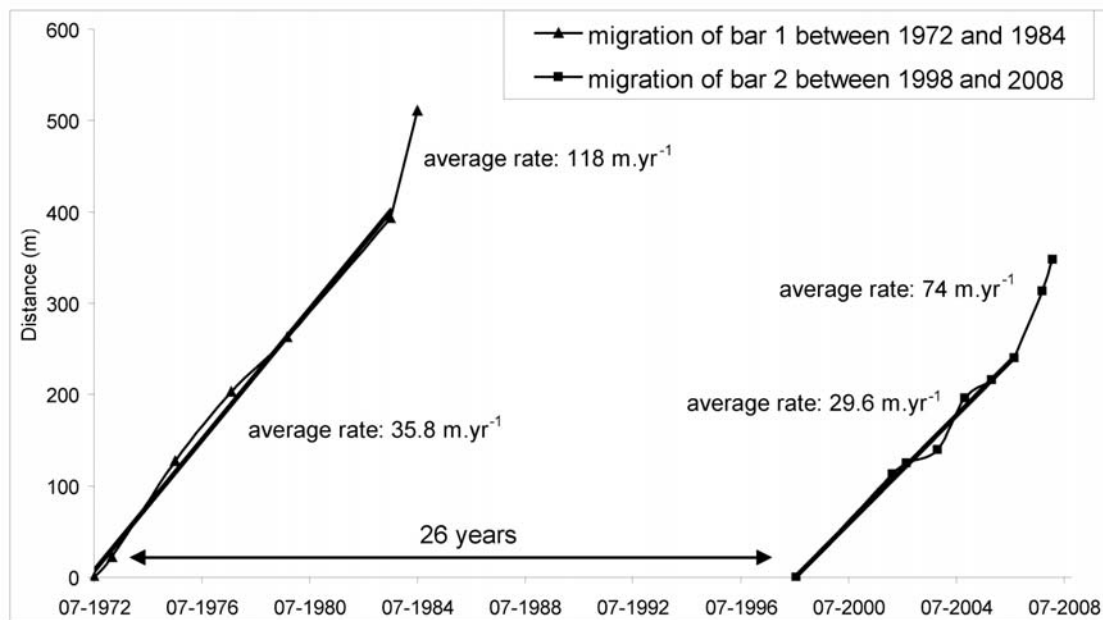


**Figure 7.** Distances covered by migrating bars 1 and 2 over the periods 1972–1984 and 1998–2008.

surveys, in November 2003, showed that bar 2 was 100 m wide, 250 m long, and 2 m high. The average migration rate toward the east-southeast, calculated from the aerial photographs and topographic survey between August 1998 and September 2006 ( $29.6 \text{ m yr}^{-1}$ ) was slightly less than that of bar 1 between 1972 and 1983 ( $35.8 \text{ m yr}^{-1}$ ) (Figure 7). This rate increased significantly, however, to attain  $74 \text{ m yr}^{-1}$  from September 2006 to February 2008, and observations subsequent to this date highlight a rate exceeding  $100 \text{ m yr}^{-1}$ . As in the case of bar 1 in 1977, swash bar 2 developed into a transverse feature in March 2005, 7 years after it was first observed on the delta. The successive phases of development of this transverse bar are highlighted by digital elevation models (Figure 8) constructed from topographic surveying of the  $700 \times 700 \text{ m}$  plot in Figure 2a.

[13] The pattern of evolution of the high-tide beach in the wake of the bar impingement and welding is depicted in Figure 9. The pattern is extracted from aerial photograph analysis (and from the post-November 2003 topographic surveys) of the shoreline updrift of the bar up to point 0 m in Figure 2a. It evinces relatively homogeneous and minor change since 2002. A global advance of the order of 10 m occurred over the 6-year period to 2008, with a hiatus of +7 m between May 2006 and February 2007 compared to the other surveys ( $\pm 2 \text{ m}$ ). The vegetation line at the lee of the bar (between 1160 m and 2000 m downdrift of point 0) showed a 60-m advance over this 6-year period. The accretion zone migrated from the 1580 m point downdrift of point 0 in 2005, to the 1640 m point in 2007, and the 1680 m point in 2008 (Figure 9). In contrast, the extremity of the spit downdrift of this accretion zone showed strong erosion (maximum of 20 m in 6 years). This appears to be an erosion hot spot, constantly in erosion in all the surveys, with a maximum of  $-14 \text{ m}$  from February 2004 to February 2005, and  $-9 \text{ m}$  between February 2005 and May 2006. This erosion was still prevalent in February 2008 (Figure 9). To summarize, since March 2004, the limit of the high-tide

beach updrift of the bar has prograded 47 m on average, while receding in the downdrift sector by about 36 m.

## 5. Discussion

### 5.1. Characteristics of Megatidal Swash Bars

[14] Two swash bars associated with an ebb tidal delta, and monitored, respectively, over the periods 1972–1992 and 1998–2008, showed relatively identical behavior that may suggest that the morphodynamic patterns observed in the vicinity of the megatidal Regnéville inlet are quite representative of this site. The bars migrated toward the shore at average speeds of  $29 \text{ m yr}^{-1}$  (bar 2) and  $35 \text{ m yr}^{-1}$  (bar 1) (Figure 7). In the course of this migration, they evolved into transverse forms relative to the shoreline. The migration showed significant acceleration in the year prior to welding onto the high-tide beach, with respective values of 118 m for bar 1 from 1983 to 1984, and 74 m for bar 2 from 2007 to 2008 (Figure 7). The migration of the bars over the ebb delta was accompanied by a reduction in their length and volume.

[15] The morphological changes and variations in migration speed exhibited by these bars indicate strong feedback relationships involving sand supply alongshore, shoreline orientation, the ebb delta platform and the hydrodynamic conditions. The behavior of these megatidal bars cannot be readily compared to that of swash bars in environments with weaker tidal ranges because the morphodynamics of the former are influenced by factors that fluctuate much more significantly over space and time than in the case of the latter. These factors include tidal prism, in part hinged on tidal range, tide-modulated wave heights, rates of longshore sediment transport, and the position of bar formation on the delta. The bars appear to be the manifestations of joint onshore and oblique downdrift sand supply from the shore face to the coastal longshore drift system updrift of the inlet. In the vicinity of the ebb delta, these bars progressively

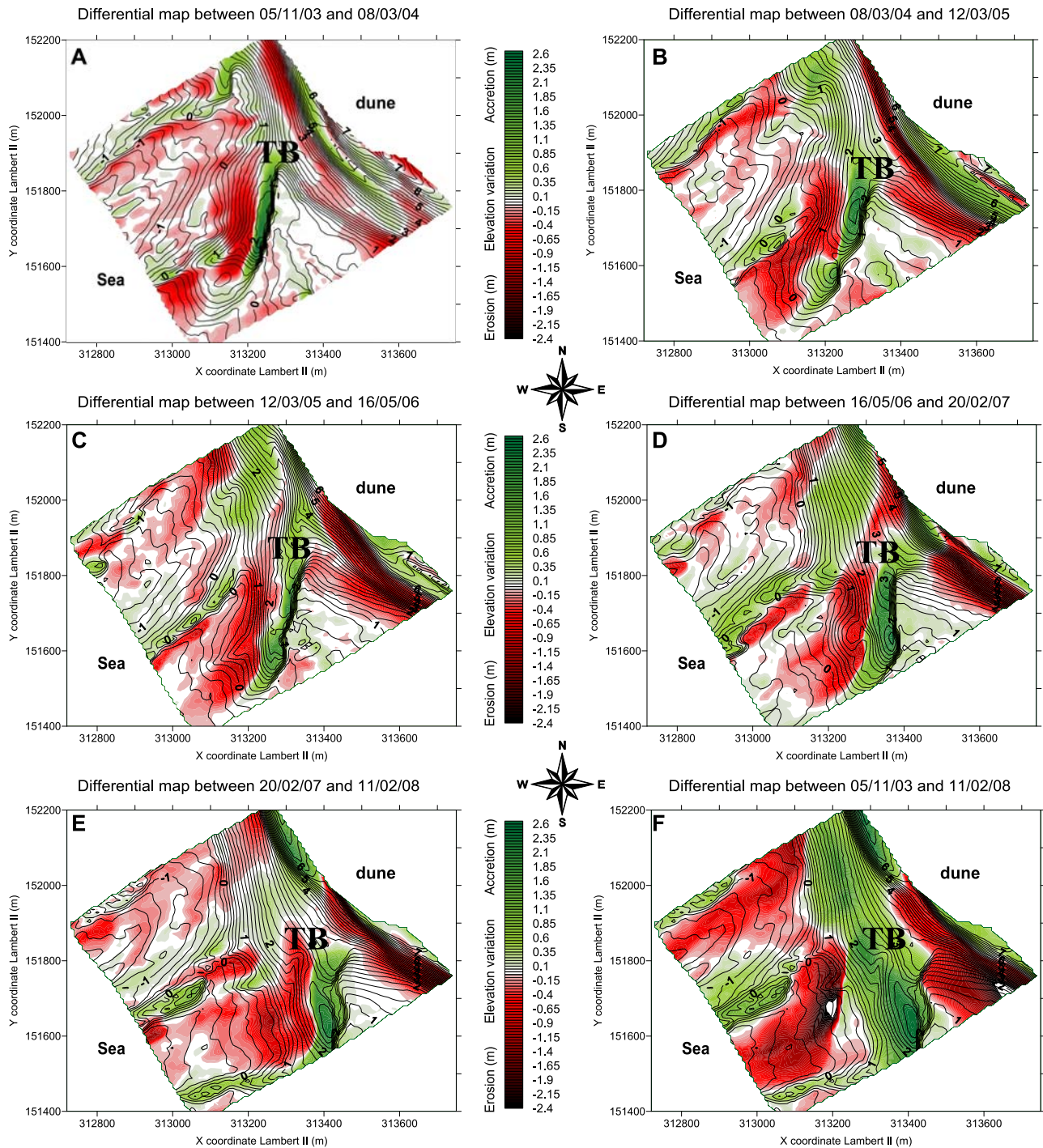


**Figure 8.** Differential digital elevation models between November 2003 and February 2008 showing the migration of swash bar 2 (TB, transverse bar).

develop as bolder swash features under the increasingly shallower water depths, emerging as transverse bars as they impinge on the ebb platform. In such large tide range settings, the net result of the tidal fluctuations is to reduce the duration over which sediment transport and morphological change occur, as suggested by *Davis et al.* [1972], who identified decreasing bar migration speeds with increasing tidal ranges. In the study area, the swash bar crest being close to the mean neap high tide level, the duration of action of all hydrodynamic processes during a tidal cycle is short

(about 2 h during neap tides and 4 h during spring tides). This low duration of bar exposure to hydrodynamic processes contributes to the low migration speeds. It has been shown that the migration speeds of the bars near Regnéville inlet are dependent on wave energy [*Robin et al.*, 2007b]. These authors showed that the bar acts as an attenuator of waves that becomes all the more effective as water depth over the bar crest diminishes. The significant dissipation of energy, particularly at neap tides (Figure 3), practically precludes wave breaking on the high-tide beach behind

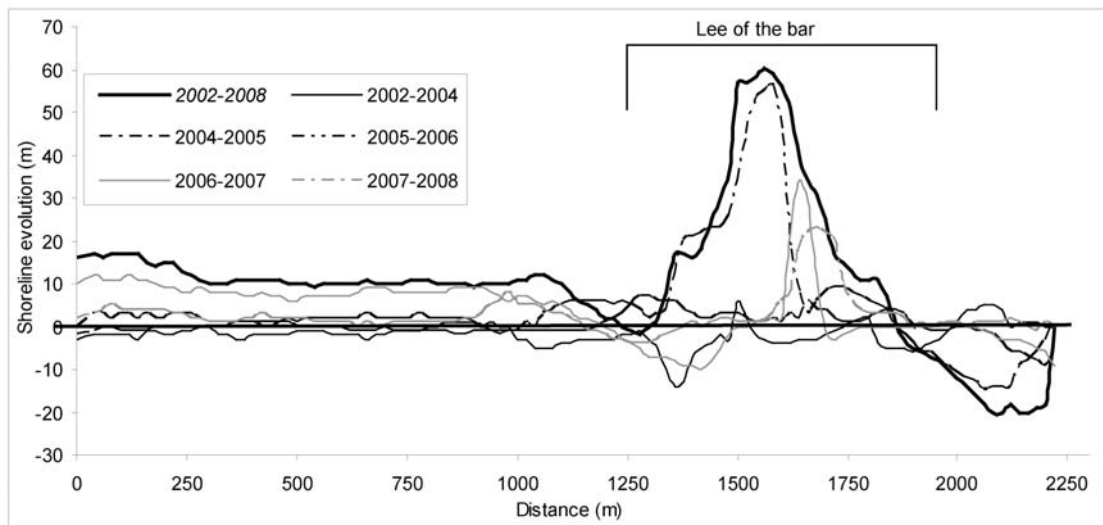


**Figure 9.** Evolution of the shoreline between 2002 and 2008 under the influence of swash bar impingement. The origin of the abscissa is shown in Figure 2a.

the bar. In contrast, the dissipative role of the bar is less pronounced at spring tides, resulting in wave breaking, and in the generation of surf and swash processes on the high-tide beach [Robin *et al.*, 2009]. Although this attenuation effect may be lessened by the conjunction of spring tides with storm events, such a conjunction remains exceptional. High-tide water depths less than 2.5 m over the crest of the bar were shown by Robin *et al.* [2007b] to represent no less than 46% of the annual tides.

[16] Apart from volume differences, described below, the patterns and rates of migration in space and time differ, compared to settings with low tidal ranges, as do the morphologies generated by onshore welding. Despite a smaller volume, the migration speed of the bars in Normandy is weaker than in other sites in the world with lower tidal ranges (e.g., 64–86 m yr<sup>-1</sup> [Smith and FitzGerald, 1994]; 133–327 m yr<sup>-1</sup> [FitzGerald, 1984]; 46 m.month<sup>-1</sup> [Balouin *et al.*, 2004]). The migration speeds of bars in the megatidal setting of Regnéville inlet accelerated before welding onto the high-tide beach, whereas the migration speeds of bars monitored by FitzGerald [1984, 1988] in a microtidal to weakly mesotidal setting decelerated as bars approached the high-tide beach due to lesser exposure to waves. Working on intertidal sand bodies (not inlet vicinity swash bars) in a megatidal embayment in Alaska, Adams *et al.* [2007] also identified pulses in migration speeds that they related to wave energy variations. The acceleration of bar migration speeds in Normandy is probably due to larger wave energy at high tide as the bar approaches the high-tide beach. Megatidal beaches, including those adjacent to the inlet, experience a significant increase in wave energy as the tide rises [Anthony *et al.*, 2004], with beach domains ranging from a dissipative to ultradissipative low-tide beach to a reflective high-tide beach [Levoy *et al.*, 2000]. The acceleration of bar 2 observed between September 2006 and February 2008, and subsequently, may also have been enhanced by more energetic wave activity, notably during spring tides, but there are no wave statistics to validate this assumption.

[17] Finally, megatidal ebb delta bars are generally small and their size decreases in the course of their migration over

the ebb delta. In contrast, in weaker tide range settings, the bars tend to coalesce to form a large complex bar [Hine, 1975, 1979; Aubrey and Speer, 1984; FitzGerald, 1984, 1988; Kana *et al.*, 1999; FitzGerald *et al.*, 1984, 2000]. The volume difference can be explained by two effects: (1) dispersal of some of the sediment locked in the megatidal swash bar over the ebb platform under the combined effect of waves and strong tidal currents and (2) the duration of tidal inundation which limits the overall time of sediment transport necessary to build the bar. However, an additional factor may be the rate at which sediment is delivered along shore to the ebb delta and across shore to the beach. This rate is expected to be higher along narrow, microtidal wave-dominated surf zones than in larger megatidal surf zones where it may be limited by the large rates of vertical and horizontal tidal translation across the wide foreshore. Macrotidal to megatidal beaches have also been shown to be characterized by relatively weak cross-shore sand transport [e.g., Anthony *et al.*, 2004, 2005; Sedrati and Anthony, 2007], and this must limit the potential sedimentary input into the bar system, and, therefore, the mean bar volume. As a result, only few bars are present on the ebb delta, and they are generally linear and of low elevation (<0.5 m). Moreover, at Agon Spit, bars tend to migrate at relatively constant speeds, thus possibly precluding the bar coalescence evoked above, and which, in microtidal or mesotidal environments, is caused by the slowing down of the migration process over the delta. An additional site-specific factor that may explain the low volumes of bars in Regnéville inlet is that of the sand-deficient nature of the shore face close to this inlet. Due to the intense offshore tidal currents, the seabed has, in the course of the Holocene, undergone winnowing of fine sand susceptible to source inlet bars, ebb deltas and coastal dunes [Anthony, 2002], and is now dominated by coarse sand and gravel [Larsonneur *et al.*, 1982].

## 5.2. Onshore Megatidal Swash Bar Migration and Shoreline Evolution: A Conceptual Model

[18] A conceptual model for the cyclic shoreline erosion and deposition generated by interactivity between an ebb

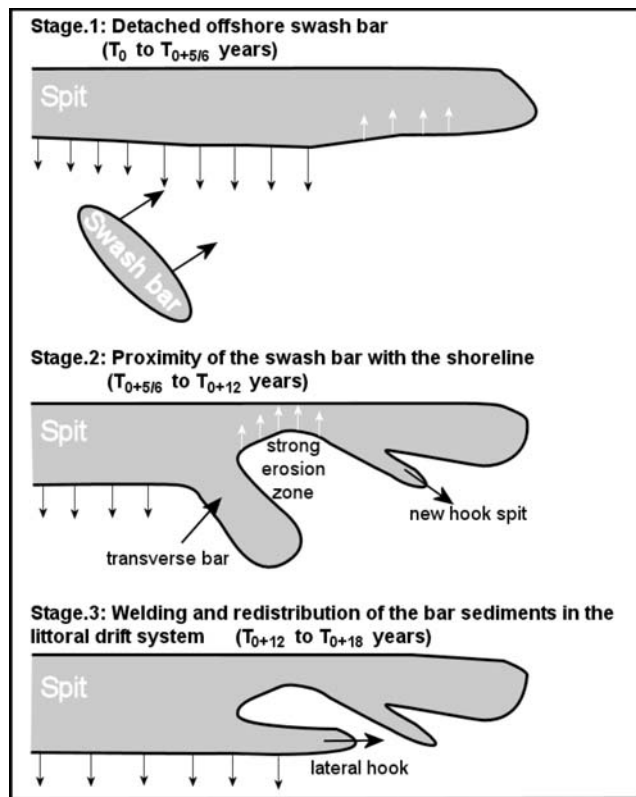


**Figure 10.** Conceptual model of shoreline changes induced by the onshore migration of a swash bar in the vicinity of a megatidal inlet.

tidal swash bar and the beach in a megatidal environment is presented in Figure 10.

### 5.2.1. Stage 1: Detached Offshore Swash Bar ( $T_0$ to $T_{0+5/6}$ Years)

[19] Between  $T_0$  and  $T_{0+5}$  years, a general progradation of the high-tide beach and of the shoreline is noticed at the updrift side of bar 1 and in the immediate leeward zone. This sequence is repeated with swash bar 2 ( $T_0$  to  $T_{0+6}$  years). Present on the ebb tidal delta hundreds of meters from the shoreline, the swash bar acts as a dissipator of waves from the west and northwest, generally the directions with the highest waves. The bar promotes stability, and then accretion of the shoreline in its shelter, especially when it is close to the high-tide beach.

### 5.2.2. Stage 2: Proximity of the Swash Bar With the Shoreline ( $T_{0+5/6}$ to $T_{0+12}$ Years)

[20] The proximity of the bar relative to the high-tide beach results in wave refraction and diffraction that significantly disrupt the longshore sediment transport. These wave transformation processes are associated with the development of a transverse bar form (submersible at high tide) that links up the swash bar from the upper midtide zone to the high-tide beach. This morphology reinforces the impact of the bar on the longshore drift system. This influence is perceptible in the evolution of the high-tide beach observed between  $T_{0+5}$  and  $T_{0+7}$  years (bar 1). The slowing down of sediment transport in the shelter of the bar promotes accretion of the high-tide beach that, in turn, has a feedback effect in reinforcing wave energy dissipation. This leads to progressive updrift migration of the accretion zone, in a counterdrift

direction on the Cotentin coast, given the dominant (net) north-south sediment transport on this coast [Levoy *et al.*, 1997]. The lee and downdrift zones become less nourished, thus resulting in the erosion of the high-tide beach and in shoreline recession. Between  $T_{0+7}$  and  $T_{0+12}$  years (bar 1), accretion of the high-tide beach and of the shoreline is enhanced updrift of the bar while erosion occurs in the downdrift sector. During this stage, the bar constitutes a strong controlling force on the evolution of the high-tide beach and leads to a significant reduction of the sediment drifting alongshore from the north (updrift end). Enhanced erosion in the downdrift sector induces a change in shoreline orientation at the distal part of the spit. This change in orientation is at the origin of the formation of a new hook spit [Robin and Levoy, 2007]. The recent morphodynamic behavior of Agon spit, between  $T_{0+6}$  and  $T_{0+10}$  (2008) (bar 2) is in agreement with this pattern. During this stage, the bar acts as an important wave energy dissipator (as in stage 1), but this is of secondary importance compared to the more significant effect of the bar on longshore drift perturbation.

### 5.2.3. Stage 3: Bar Welding and Redistribution of Bar Sediments in the Littoral Drift System ( $T_{0+12}$ to $T_{0+18}$ Years)

[21] From  $T_{0+12}$  to  $T_{0+18}$  years (bar 1), the bar becomes fully integrated in the morphodynamics of the high-tide beach and participates in the formation of a lateral hook, parallel to the shoreline. At this stage, the north-south sediment transport is no longer slowed down and becomes virtually normal once again. The elongation of the lateral hook actively continues until the latter joins the terminal hook years later. After  $T_{0+18}$  years, the sediment transport at Agon spit is no longer disrupted and the terminal hook grows quickly downdrift south-southeastward. The formation of a new bar (2) on the ebb tidal delta in  $T_{0+26}$  years marks the beginning of a new cycle.

## 5.3. Comparison of Megatidal Tidal Inlet Shoreline Behavior With That of Micromesotidal Environments

[22] At Agon spit, stage one of the conceptual model proposed in the present study is similar to patterns from the models of Hine [1979] and Kana *et al.* [1999]. Stage 2 is, however, characterized by updrift accretion and by strong erosion at the downdrift sector of the swash bar, and this constitutes an original pattern. Because of low migration rates, the time of presence of the bar near the high-tide beach is much larger in megatidal environments ( $\sim 7$  years for bar 1 (1977–1984) and at least 4 years for bar 2 (2004–2008, with a welding phase that is still ongoing) than on coasts with smaller tidal ranges (approximately 1 year). This explains the strong disturbance such bars induce in the sediment dynamics of the high-tide beach and in shoreline evolution in large tide range environments, it also explains the longer cycle of migration and welding of swash bars [Robin and Levoy, 2007]. The transverse bar morphology observed in 1977 for bar 1, and since 2005 for bar 2, also testifies to the influence of these forms on sediment transport on the high-tide beach. Unlike lower tide range environments, where swash bars source the formation of new hook spits, as in the Hine [1979] model of berm development, swash bars in the megatidal setting do not become the new hook spit. Their

sediment is reorganized in the longshore drift system through the formation and progradation of a lateral hook.

## 6. Conclusion

[23] Interpretation of results obtained from the analysis of vertical aerial photographs over a timescale of years, combined with short-term field experiments, highlights original features of the relationship between swash bars and the shore in a megatidal setting, thus complementing efforts that have been virtually exclusively directed at the analysis of this relationship in microtidal to mesotidal environments. A number of conclusions can be drawn from this study:

[24] 1. A close relation exists between the position of the swash bar on the ebb tidal delta and the general dynamics of the shoreline. When located in the midtide zone, the bar protects the shoreline, promoting general progradation of the high-tide beach and of the shoreline at the updrift side of the bar and just behind it, in a sediment system controlled by the longshore transport. When located near the high-tide beach, part of the bar evolves into a submerged transverse feature that acts as an obstacle to the longshore transport. The bar disrupts the north-south sediment transport, thus facilitating accretion updrift and erosion downdrift of the bar.

[25] 2. The relationship observed between the position of the swash bar and shoreline evolution is linked with the tidal characteristics of the field site. High-tide water depths over the top of the bar vary significantly between neap (0.8 m) and spring (4–4.5 m) tides. During neap tides, most of the wave energy is dissipated, thus highlighting the influence of the bar on wave propagation. The bar influence becomes insignificant when water depths exceed 2.5 m, during spring tides. The presence of a bar in the midtide zone is thus a factor of stability of the beach and of the shoreline. The large tidal water level fluctuation results in a short duration of bar reworking compared to micro-mesotidal environments with similar wave energy levels. The large tidal excursion rates favor slow bar migration, and this leads to longer persistence of the perturbing influence of the bar on the littoral drift system and on shoreline dynamics, especially when the bar is located near the high-tide beach.

[26] 3. Swash bars in the megatidal environment of Normandy seem to be characterized by relatively small volumes (29,000 m<sup>3</sup>) and by a long cycle of migration and welding (26 years), in contrast to bars evolving in micro-mesotidal environments, where wave-dominated processes generate potentially active longshore sediment transport, active swash bar formation and migration, and bar coalescence that may significantly source beach accretion. In the megatidal setting described here, swash bar welding onto the beach is an insignificant source of mesoscale to long-term sand supply to the beach, compared to the littoral drift potential (40,000 m<sup>3</sup> yr<sup>-1</sup>).

[27] **Acknowledgments.** This work is part of the Ph.D. thesis of N.R. carried out under the supervision of F.L. The project was supported by the Conseil Régional de Basse-Normandie, the Conservatoire du Littoral, and the Agence de l'Eau. We thank Julia Bastide, Laurent Benoit, Jean Michel Couton, and Franck Lelong for their constant support in the field and Guillaume Izabel for drawing the figures. Three anonymous reviewers are thanked for their constructive suggestions for improvement.

## References

- Adams, P. N., P. Ruggiero, G. C. Schoch, and G. Gelfenbaum (2007), Intertidal sand body migration along a megatidal coast, Kachemak Bay, Alaska, *J. Geophys. Res.*, *112*, F02007, doi:10.1029/2006JF000487.
- Anthony, E. J. (2002), Long-term marine bedload segregation, and sandy versus gravelly Holocene shorelines in the eastern English Channel, *Mar. Geol.*, *187*, 221–234, doi:10.1016/S0025-3227(02)00381-X.
- Anthony, E. J., F. Levoy, and O. Monfort (2004), Morphodynamics of intertidal bars on a megatidal beach, Merlimont, northern France, *Mar. Geol.*, *208*, 73–100, doi:10.1016/j.margeo.2004.04.022.
- Anthony, E. J., F. Levoy, O. Monfort, and C. Degryse-Kulkarni (2005), Short-term intertidal bar mobility on a ridge-and-runnel beach, Merlimont, northern France, *Earth Surf. Processes Landforms*, *30*, 81–93, doi:10.1002/esp.1129.
- Anthony, E. J., S. Vanhée, and M. H. Ruz (2007), Embryo dune development on a large, actively accreting macrotidal beach: Calais, North Sea coast of France, *Earth Surf. Processes Landforms*, *32*, 631–636, doi:10.1002/esp.1442.
- Aubrey, D. G., and P. E. Speer (1984), Updrift migration of tidal inlets, *J. Geol.*, *92*, 531–546, doi:10.1086/628890.
- Aubry, A., S. Lesourd, A. Gardel, P. Dubuisson, and M. Jeanson (2009), Sediment textural variability and mud storage on a large accreting sandflat in a macrotidal, storm-wave setting: The North Sea coast of France, *J. Coastal Res., Spec. Issue*, *56*, 163–167.
- Balouin, Y., H. Howa, and D. Michel (2001), Swash platform morphology in the ebb-tidal delta of the Barra Nova inlet, south Portugal, *J. Coastal Res.*, *17*, 784–791.
- Balouin, Y., B. D. Bradley, M. A. Davidson, and H. Howa (2004), Morphology evolution of an ebb-tidal delta following a storm perturbation: Assessments from remote sensed data and direct surveys, *J. Coastal Res.*, *20*, 415–424, doi:10.2112/1551-5036(2004)020[0415:MEOAED]2.0.CO;2.
- Boak, E. H., and I. L. Turner (2005), Shoreline definition and detection: A review, *J. Coastal Res.*, *21*, 688–704, doi:10.2112/03-0071.1.
- Borrelli, M., and J. T. Wells (2003), Swash bars and spits growth: Evolution of a rapidly prograding spit along a sediment-starved coast, paper presented at Coastal Sediment '03 Conference, Am. Soc. of Civ. Eng., St. Petersburg, Fla.
- Crowell, M., S. P. Leatherman, and M. K. Buckley (1991), Historical shoreline change: Error analysis and mapping accuracy, *J. Coastal Res.*, *7*, 839–852.
- Davis, R. A., Jr. (2004), Tidal influence on barrier island morphodynamics: Examples from Florida, USA, *J. Coastal Res., Spec. Issue*, *39*, 97–101.
- Davis, R. A., W. T. Fox, M. O. Hayes, and J. C. Boothroyd (1972), Comparison of ridge and runnel systems in tidal and non-tidal environments, *J. Sediment. Petrol.*, *42*, 413–421.
- Fenster, M., and R. Dolan (1996), Assessing the impact of tidal inlets on adjacent barrier island shorelines, *J. Coastal Res.*, *12*, 294–310.
- Fisher, J. S., and M. F. Overton (1994), Interpretation of shoreline position from aerial photographs, paper presented at 24th International Conference on Coastal Engineering, Am. Soc. of Civ. Eng., Kobe, Japan.
- FitzGerald, D. M. (1982), Sediment bypassing at mixed energy tidal inlets, paper presented at 18th International Conference on Coastal Engineering, Am. Soc. of Civ. Eng., Cape Town, South Africa.
- FitzGerald, D. M. (1984), Interactions between the ebb-tidal delta and landward shoreline: Price Inlet, South Carolina, *J. Sediment. Petrol.*, *54*, 1303–1318.
- FitzGerald, D. M. (1988), Shoreline erosional-depositional processes associated with tidal inlets, in *Hydrodynamics and Sediment Dynamics of Tidal Inlets, Lect. Notes Coastal Estuarine Stud.*, vol. 29, edited by D. G. Aubrey and L. Weishar, pp. 186–224, Springer, New York.
- FitzGerald, D. M., S. Penland, and D. Nummedal (1984), Control of barrier island shape by inlet sediment bypassing: East Frisian Islands, west Germany, *Mar. Geol.*, *60*, 355–376, doi:10.1016/0025-3227(84)90157-9.
- FitzGerald, D. M., N. C. Kraus, and E. B. Hands (2000), Natural mechanisms of sediment bypassing at tidal inlets, *Coastal Hydraul. Eng. Tech. Note ERDC/CHL CETN-IV-30*, U.S. Army Eng. Res. and Dev. Cent., Vicksburg, Miss.
- Gaudiano, D. J., and T. W. Kana (2001), Shoal bypassing in mixed energy inlets: Geomorphic variables and empirical predictions for nine South Carolina inlets, *J. Coastal Res.*, *17*, 280–291.
- Hayes, M. O. (1975), Morphology and sand accumulation in estuaries, in *Estuarine Research*, vol. 2, *Geology and Engineering*, edited by L. E. Cronin, pp. 3–22, Academic, San Diego, Calif.
- Hicks, D. M., T. M. Hume, A. Swales, and M. O. Green (1999), Magnitudes, spatial extent, time scales and causes of shoreline change adjacent to an ebb tidal delta, Katikati inlet, New Zealand, *J. Coastal Res.*, *15*, 220–240.
- Hine, A. C. (1975), Bedform distribution and migration pattern on tidal deltas in the Chatman Harbor Estuary, Cape Cod, Massachusetts, in

- Estuarine Research*, vol. 2, *Geology and Engineering*, edited by L. E. Cronin, pp. 235–252, Academic, San Diego, Calif.
- Hine, A. C. (1979), Mechanisms of berm development and resulting beach growth along a barrier spit complex, *Sedimentology*, 26, 333–351, doi:10.1111/j.1365-3091.1979.tb00913.x.
- Kana, T. W., and P. M. McKee (2003), Relocation of Captain Sams Inlet – 20 years later, paper presented at Coastal Sediment '03 Conference, Am. Soc. of Civ. Eng., St. Petersburg, Fla.
- Kana, T. W., M. L. Williams, and D. Stevens (1985), Managing shoreline changes in the presence of nearshore shoal migration and attachment, in *Proceedings of the Fourth Symposium on Coastal and Ocean Management*, edited by O. T. Magoon et al., pp. 1277–1294, Am. Soc. of Civ. Eng., New York.
- Kana, T. W., E. J. Hayter, and P. A. Work (1999), Mesoscale sediment transport at southeastern U.S. tidal inlets: Conceptual model applicable to mixed energy settings, *J. Coastal Res.*, 15, 303–313.
- Larsonneur, C., P. Bouysse, and J. P. Auffret (1982), The superficial sediments of the English Channel and its western approaches, *Sedimentology*, 29, 851–864, doi:10.1111/j.1365-3091.1982.tb00088.x.
- Levoy, F. (1994), Evolution et fonctionnement hydrosédimentaire des plages macrotidales—L'exemple de la côte ouest du Cotentin, Ph.D. thesis, 424 pp., Univ. of Caen, Caen, France.
- Levoy, F., O. Monfort, and C. Larsonneur (1997), Transport solides sur les plages macrotidales: Traçage fluorescent et application à la côte ouest du Cotentin (France), *Oceanol. Acta*, 20, 811–822.
- Levoy, F., E. J. Anthony, O. Monfort, and C. Larsonneur (2000), The morphodynamics of megatidal beaches in Normandy, France, *Mar. Geol.*, 171, 39–59, doi:10.1016/S0025-3227(00)00110-9.
- Levoy, F., O. Monfort, and C. Larsonneur (2001), Hydrodynamic variability on megatidal beaches, Normandy, France, *Cont. Shelf Res.*, 21, 563–586, doi:10.1016/S0278-4343(00)00128-X.
- Moore, L. J. (2000), Shoreline mapping techniques, *J. Coastal Res.*, 16, 111–124.
- Moore, L. J., C. Sullivan, and D. G. Aubrey (2003), Interannual evolution of multiple longshore sand bars in a mesotidal environment, Truro, Massachusetts, USA, *Mar. Geol.*, 196, 127–143, doi:10.1016/S0025-3227(03)00028-8.
- Nummedal, D., and S. Penland (1981), Sediment dispersal in Norderney Seegat, West Germany, in *Proceedings of National Meeting on Holocene Marine Sedimentation in the North Sea Basin*, Spec. Publ. Int. Assoc. Sedimentol., 5, 187–210.
- Oertel, G. F. (1972), Sediment transport of estuary entrance shoals and the formation of swash platforms, *J. Sediment. Petrol.*, 42, 858–868.
- Oertel, G. F. (1977), Geomorphic cycles in ebb deltas and related patterns of shore erosion and accretion, *J. Sediment. Petrol.*, 47, 1121–1131.
- Parker, B. B. (2003), The difficulties in measuring a consistently defined shoreline: The problem of vertical referencing, *J. Coastal Res.*, Spec. Issue 38, 44–56.
- Reichmüth, B., and E. J. Anthony (2007), Tidal influence on the intertidal bar morphology of two contrasting macrotidal beaches, *Geomorphology*, 90, 101–114, doi:10.1016/j.geomorph.2007.01.015.
- Robin, N. (2007), Morphodynamique des systèmes de flèches sableuses: Etude entre les embouchures tidales de l'Archipel de St Pierre et Miquelon et de la côte ouest du Cotentin (Manche), Ph.D. thesis, 529 pp., Univ. of Caen, Caen, France.
- Robin, N., and F. Levoy (2005), Morphodynamics of bars on the ebb delta of a megatidal inlet (Normandy, France), paper presented at 5th International Conference on Coastal Dynamics, Am. Soc. of Civ. Eng., Barcelona, Spain.
- Robin, N., and F. Levoy (2007), Etapes et rythmes de formation d'une flèche sédimentaire à crochets multiples en environnement megatidal, *Z. Geomorphol.*, 51, 337–360, doi:10.1127/0372-8854/2007/0051-0337.
- Robin, N., F. Levoy, and O. Monfort (2007a), Formation and evolution of a complex spit in megatidal environment, Agon Spit (Normandy, France), paper presented at 25th IAS Meeting of Sedimentology, Int. Assoc. of Sedimentol., Patras, Greece, 4–7 Sept.
- Robin, N., F. Levoy, and O. Monfort (2007b), Bar morphodynamic behaviour on the ebb delta of a macrotidal inlet (Normandy, France), *J. Coastal Res.*, 23, 1370–1378, doi:10.2112/06-0684.1.
- Robin, N., F. Levoy, and O. Monfort (2009), Short term morphodynamics of an intertidal bar on megatidal ebb delta, *Mar. Geol.*, 260, 102–120, doi:10.1016/j.margeo.2009.02.006.
- Russell, P., M. Davidson, D. Huntley, A. Cramp, J. Hardisty, and G. Lloyd (1991), The British beach and nearshore dynamics (B-BAND) programme, in *Proceedings of a Specialty Conference on Quantitative Approaches to Coastal Sediment Processes*, edited by N. C. Kraus et al., pp. 371–384, Am. Soc. of Civ. Eng., New York.
- Sedrati, M., and E. J. Anthony (2007), Storm-generated morphological change and longshore sand transport in the intertidal zone of a multi-barred macrotidal beach, *Mar. Geol.*, 244, 209–229, doi:10.1016/j.margeo.2007.07.002.
- Smith, J. B., and D. M. FitzGerald (1994), Sediment transport at the Essex River inlet ebb-tidal delta, Massachusetts, USA, *J. Coastal Res.*, 10, 752–774.
- Voulgaris, G., T. Mason, and M. B. Collins (1996), An energetics approach for suspended sand transport on macrotidal ridge and runnel beaches, paper presented at 25th International Coastal Engineering Conference, Am. Soc. of Civ. Eng., Orlando, Fla.

E. Anthony, Laboratoire d'Océanologie et de Géosciences, UMR 8187, Université du Littoral Côte d'Opale, CNRS, 32, av. Foch, F-62930 Wimereux, France.

F. Levoy, O. Monfort, and N. Robin, Laboratoire Morphodynamique Continentale et Côtère, UMR 6143, Université de Caen, CNRS, 2-4 rue des tilleuls, F-14000 Caen, France. (nicolas.robin@univ-perp.fr)